Computer Aided Civil and Infrastructure Engineering, in review.
Web version at http://rcf.usc.edu/~johnsone/papers/smartdamping_sagcable.html

SEMIACTIVE DAMPING OF CABLES WITH SAG

E.A. Johnson,[1] R.E. Christenson,[2] and B.F. Spencer, Jr.[3]

[1] Department of Civil Engineering, University of Southern California,
Los Angeles, CA 90089-2531, USA
[2] Division of Engineering, Colorado School of Mines,
Golden, CO 80401, USA
[3] Department of Civil Engineering and Geological Sciences, University of
Notre Dame, Notre Dame, IN 46556-0767, USA

ABSTRACT

Cables, such as are used in cable-stayed bridges, suspension bridges, guy wires, transmission lines, and flexible space structures, are prone to vibration due to their low inherent damping characteristics. The mitigation of cable vibration is necessary to minimize negative impact. Transversely-attached passive viscous dampers have been implemented on some cables to dampen vibration. However, it can be shown that only minimal damping can be added if the damper attachment point is close to the end of the cable. For long cables, passive dampers may provide insufficient supplemental damping to eliminate vibration problems. A recent study by the authors demonstrated that "smart" semiactive damping can provide significantly superior supplemental damping for a cable modeled as a taut string. This paper extends the previous work by adding sag, inclination, and axial flexibility to the cable model. The equations of motion are given. A new control-oriented model is developed for cables with sag. Passive, active, and smart (semiactive) dampers are incorporated into the model. Cable response is seen to be dramatically reduced by semiactive dampers for a wide range of cable sag and damper location.

KEYWORDS

semiactive damping, rain-wind induced vibration, cable sag, structural control

INTRODUCTION

Cables are efficient structural elements that are used in cable-stayed bridges, suspension bridges and other cable structures. These cables are subject to environmental excitations, such as rain-wind induced vibration, and support excitations. Steel cables are flexible and have low inherent damping (Yamaguchi and Fujino, 1998), resulting in high susceptibility to vibration. Vibration can result in premature cable or connection failure and/or breakdown of the cable corrosion protection systems, reducing the life of the cable structure (Watson and Stafford, 1988). Additionally, cable vibrations can have a detrimental effect on public confidence in the safety of cable structures. Transmission lines have also demonstrated signif-

icant vibration problems, including those caused by vortex shedding, wake-induced oscillation, and iced and ice-free galloping. Fatigue of the transmission lines near clamps or masses (such as aircraft warning spheres) is the principal effect of conductor vibration, though galloping can cause sparkover between lines of different phase (Tunstall, 1997).

A number of methods have been proposed to mitigate cable vibrations. For stay cables, tying cables together, aerodynamic cable surface modification, and passive and active axial and transverse cable control have been used to dampen vibration. Tying cables together shortens the cables and is intended to shift the frequencies of the cable out of the range of the excitation. This strategy deteriorates the aesthetics of the cable structure. Changing the surface of the cable to reduce susceptibility to environmental excitations has also been explored, but is impractical for retrofit applications and may increase the drag on the cable (Yamaguchi and Fujino, 1998). For transmission lines, two primary methods are used for reducing vibration. Stockbridge dampers (Stockbridge, 1925), a variety of tuned vibration absorbers, are the most common means today for adding supplemental damping to transmission lines (Tunstall, 1997). An alternate solution for multiple parallel transmission lines is adding dampers to the bundle spacers routinely used for separating conductors (Edwards and Boyd, 1965).

A number of researchers have proposed passive control of cables using viscous dampers attached transverse to the cables. Kovacs (1982) first identified that an optimal damper size exists and developed optimal damping coefficients for the transverse passive viscous damper control strategy of a taut cable. Sulekh (1990) and Pacheco *et al.* (1993) numerically developed a "universal" design curve to facilitate the design of passive dampers for stay cables. This nondimensionalized curve can be used to specify the optimal viscous damping properties for a desired mode of any given cable span and fundamental frequency. Krenk (2000) obtained explicit asymptotic results for the optimal damping coefficients, developing an analytical solution for the design curve. These studies indicate that, for a passive linear damper, the maximum supplemental damping ratio is approximately $\bar{x}_\mathrm{d}/2L$, where $\bar{x}_\mathrm{d}$ is the distance from the cable anchorage to the damper and L is the length of the cable.

Transverse passive viscous dampers have been applied to full-scale applications, including the cables on the Brotonne Bridge in France (Gimsing, 1983), the Sunshine Skyway Bridge in Florida (Watson and Stafford, 1988) and the Aratsu Bridge in Japan (Yoshimura *et al.*, 1989). The damper location is typically restricted to be close to the bridge deck for aesthetic and practical reasons. For short cables, a high $\bar{x}_\mathrm{d}/L$ ratio is feasible and a passive damper can provide sufficient damping. For longer bridge cables, such as in the planned 1100 meter main-span bridge in Hong Kong (Russell, 1999) or the Normandie and Tatara bridges with cables more than 450 meters long (Endo *et al.*, 1991; Virloguex *et al.*, 1994), passive dampers cannot provide enough supplemental damping to eliminate vibration effects, such as the rain-wind induced motion, without significant changes to the aesthetics of the structure.

Several recent papers by the authors have shown that semiactive dampers may provide levels of damping far superior to their passive counterparts. Johnson *et al.* (1999, 2000, 2002a) used a taut string model of in-plane cable vibration and developed a control-oriented model using a static deflection shape in a series expansion for the cable motion. They showed that a "smart" semiactive damper can provide 50 to 80% reduction in cable response compared to the optimal passive linear damper. The level of reduction was most significant when the damper is connected close to the cable anchorage. A passive damper moved close to the end of the cable was shown to rapidly lose any ability to add damping to the system, whereas a semiactive damper retained most of its performance even at damper locations below 1% of the cable length (though with larger forces).

The taut string model of cable vibration neglects some cable characteristics that are known to have some affect on passive damper performance. Cable sag, inclination, and axial flexibility all affect the dynam-

ics of the cable. In particular, they combine together to modify the stiffness of the modes that are symmetric about the center of the cable. Previous studies have examined the performance of transverse passive viscous dampers on sag cables. For example, using a sine series Galerkin approach, Sulekh (1990) showed that the damping added to the first symmetric mode by passive dampers was reduced by sag — by about 14% for a typical stay cable sag level — compared to that predicted by a taut string model. Further, the higher modes were virtually unaffected. An alternate approach by Xu *et al.* (1998a,b,c), using a spatial discretization, made similar observations, with a 38% decrease in first-symmetric-mode damping for a long (442.6 m) stay cable with slightly larger sag.

This study extends the aforementioned work by the authors to investigate the combined effects of cable sag, inclination, and axial flexibility on the performance of semiactive cable damping. An extension to the control-oriented model of Johnson *et al.* (2002a) is developed herein to accommodate these cable characteristics. Cables with linear passive viscous dampers, active dampers, and semiactive dampers are examined for various damper locations and for various levels of cable sag, inclination and axial flexibility. Semiactive damper performance is seen to degrade some for certain regions, but far less than their passive counterparts. Semiactive dampers are further shown to perform significantly better than passive dampers for sag, inclination and axial flexibility typical of bridge stay cables and for most larger levels of sag.

IN-PLANE MOTION OF CABLES WITH SAG

Consider the uniform cable suspended between two supports of different heights, as shown in Figure 1. This study investigates cables with a flat profile (flat-sag cables); for a horizontal cable, this requires the sag to span ratio be less than 1:8 (for inclined cables the assumption is valid but over a smaller range of sag) (Irvine, 1981). Further, the effects of longitudinal flexibility are included and flexural rigidity is ignored.† The static profile of the cable can be approximated by a parabolic curve and the in-plane transverse cable motion $w(x, t)$, relative to the static profile, is given by the nondimensional equation of motion (Irvine, 1981)

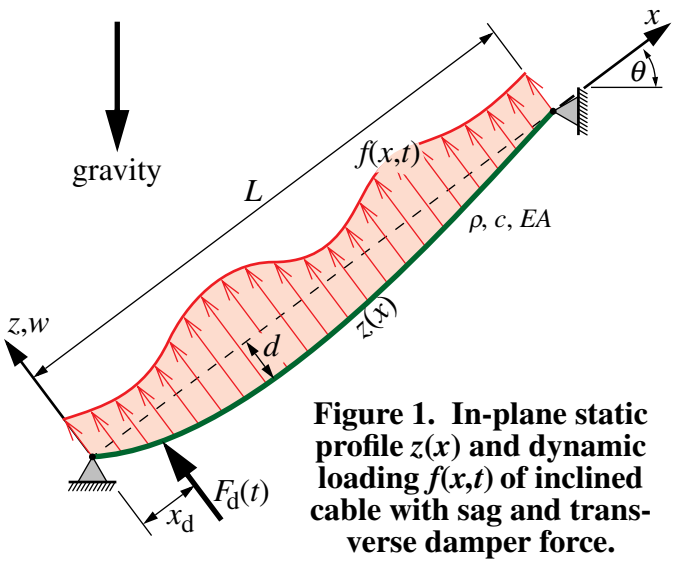

Figure 1. In-plane static profile $z(x)$ and dynamic loading $f(x,t)$ of inclined cable with sag and transverse damper force.

$$\ddot{w}(x, t) + c\dot{w}(x, t) - \frac{1}{\pi^2}w''(x, t) + \frac{\lambda^2}{\pi^2}\left[\int_0^1 w(\xi, t)d\xi\right] = f(x, t) + F_d(t)\delta(x - x_d) \qquad (1)$$

in the domain $0 \le x \le 1$, with boundary conditions $w(0, t) = w(1, t) = 0$. c is the viscous damping per unit length, $(\,)'$ and $(\dot{})$ denote partial derivatives with respect to x and t, respectively, $f(x, t)$ is the distributed load on the cable, $F_d(t)$ is a transverse in-plane damper force at location $x = x_d$, and $\delta(\cdot)$ is the Dirac delta function. The nondimensional quantities are related to their dimensional counterparts, shown with overbars, according to the following relations

† Christenson (2001) showed that flexural rigidity typical of bridge stay cables has only a small effect on the performance of transverse damping strategies.

$$t = \omega_0 \bar{t} \qquad x = \bar{x}/L \qquad c = \bar{c}/\rho\omega_0 \qquad w(x,t) = \bar{w}(\bar{x},\bar{t})/L \qquad \omega_0^2 = H\pi^2/\rho L^2$$
$$\delta(x - x_d) = L\bar{\delta}(\bar{x} - \bar{x}_d) \qquad f(x,t) = L\bar{f}(\bar{x},\bar{t})/\pi^2 H \qquad F_d(t) = \bar{F}_d(\bar{t})/\pi^2 H \tag{2}$$

where L is the length of the cable, ω_0 is the fundamental natural frequency of the undamped cable without sag, H is the component of cable tension in the longitudinal x-direction, and ρ is the cable mass per unit length. λ^2 is the nondimensional independent parameter (Irvine, 1981)‡

$$\lambda^2 = \left(\frac{\rho g L \cos\theta}{H}\right)^2 \frac{EAL}{HL_e} = 64\left(\frac{\bar{d}}{L}\right)^2 \frac{EAL}{HL_e} \tag{3}$$

where θ is the inclination angle, L_e is the static (stretched) length of the cable

$$L_e = L\left[1 + \frac{1}{8}\left(\frac{\rho g L \cos\theta}{H}\right)^2\right] = L\left[1 + 8\left(\frac{\bar{d}}{L}\right)^2\right] \tag{4}$$

For flat-sag cables,

$$\bar{d} = dL = (\rho g L^2 \cos\theta)/8H \tag{5}$$

is the peak (dimensional) sag of the parabolic static profile

$$\bar{z}(\bar{x}) = -4\bar{d}\frac{\bar{x}}{L}\left(1 - \frac{\bar{x}}{L}\right) \tag{6}$$

The effects of cable sag, angle-of-inclination, and axial stiffness on the nondimensional dynamic response of the system enter only though the independent parameter λ^2. Increasing sag increases λ^2 but increased angle of inclination and axial flexibility decrease λ^2. While one could assume variations of λ^2 are from changes in the angle-of-inclination or axial stiffness, for simplicity and clarity, this paper will, without loss of generality, refer to variations in λ^2 as varying levels of sag, though λ^2 really captures the effects of all three of these phenomena for a flat-sag cable.

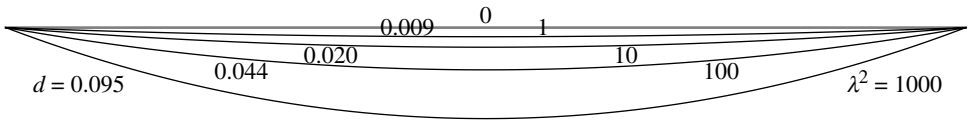

Figure 2. Typical static sag profiles.

Stay cables on cable-stayed bridges typically have λ^2 values on the order of 1 or smaller (Gimsing, 1983); some stay cables reported in the literature have larger λ^2 values such as the 2.2 reported in Pacheco *et al.* (1993) and the 3.6 reported in Xu *et al.* (1998a). Typical transmission line characteristics (Tunstall, 1997) give a λ^2 in the neighborhood of 90. $\lambda^2 \in [140, 350]$ is the range typical for the main cable on a suspension bridge (Gimsing, 1983). Specific performance examples will be given below for control of cables with some λ^2 values of interest, as well as the general trends as λ^2 increases from 0 to 500. Typical static cable profiles are shown to scale in Fig. 2 for several λ^2 values*. Even for large λ^2 values such as the $\lambda^2 = 1000$ shown, the

‡ Irvine's terminology "the independent parameter λ^2" (Irvine, 1981) is adopted herein; others have referred to λ^2 as the "nondimensional Irvine parameter," or the "nondimensional sag parameter."

* The cable parameters are taken from Pacheco *et al.* (1993) assuming steel material properties; only tension is adjusted to give the varying levels of λ^2 and sag using equations (3), (4), and (5).

midspan sag-to-length ratio d is less than the 1/8 required for the flat-sag cable (*i.e.*, parabolic static profile) assumption for horizontal cables (Irvine, 1981).

Control-Oriented Series Solution to the Nondimensional Equation of Motion

Determining an accurate and efficient control-oriented design model is the first and fundamental step in the design of a semiactive control strategy. A design model is sought that can capture the salient features of the dynamic system with a relatively small number of degrees-of-freedom (DOFs). Previous transversely-controlled cable models have employed the Galerkin method, using only sine shape functions requiring 350 DOFs (Sulekh, 1990; Pacheco *et al.*, 1993), as well as hybrid-type finite element methods which also require numerous DOFs to insure accurate results (Xu *et al.*, 1998a). Semiactive control design, as well as the computation of performance criteria through simulation with numerous control strategies, is impractical for systems of such size. Thus, successful semiactive control design is dependant on determining a lower order, control-oriented design model. This is accomplished here by including a static deflection shape in addition to the sine series in the approximation of the cable motion.

Using a Galerkin method, the motion of the cable may be computed using a finite series approximation

$$w(x,t) \;=\; \sum_{j\,=\,1}^{m} q_j(t)\,\phi_j(x) \tag{7}$$

where the $q_j(t)$ are generalized displacements and the $\phi_j(x)$ are a set of shape functions that are continuous with piecewise continuous slope and that satisfy the geometric boundary conditions

$$\phi_j(0) \;=\; \phi_j(1) \;=\; 0 \tag{8}$$

A sine series may be used for the shape functions, though Johnson *et al.* (2002a) showed that the convergence of this series is slow, making it difficult to construct a control-oriented model. However, they also demonstrated that the introduction of a static deflection shape as an additional shape function significantly improved the series convergence and provided an excellent control-oriented model. This approach is used here as well, though it must be extended to account for sag.

Consider the static deflection of a cable with sag due to a unit load at location $x \;=\; x_{\mathrm{d}}$ — the same as the equation of motion (1) without the dynamic terms and with a unit point load on the right hand side

$$-\frac{1}{\pi^2}w''_{\mathrm{static}}(x) + \frac{\lambda^2}{\pi^2}\left[\int_0^1 w_{\mathrm{static}}(\xi)\,d\xi\right] \;=\; \delta(x-x_{\mathrm{d}}) \qquad\qquad w_{\mathrm{static}}(0) \;=\; w_{\mathrm{static}}(1) \;=\; 0 \tag{9}$$

For a given deflection $w_{\mathrm{static}}(x)$, the integral term in (9) acts like a constant load distributed over the entire length of the cable. Such a load produces a parabolic deflection. The point load, given by the Dirac delta, adds a triangular component. Substituting a linear combination of parabolic and triangular deflections into (9) and solving for the unknown coefficients results in the static deflection

$$w_{\mathrm{static}}(x) \;=\; \pi^2(1-x_{\mathrm{d}})x - \pi^2(x-x_{\mathrm{d}})H(x-x_{\mathrm{d}}) - \frac{3\lambda^2\pi^2 x_{\mathrm{d}}(1-x_{\mathrm{d}})}{12+\lambda^2}x(1-x) \tag{10}$$

where $H(x - x_d)$ is the Heaviside, or unit step, function. For consistent shape function scaling, (10) is normalized to give a maximum deflection of 1,[§] resulting in the static deflection shape function

$$\phi_1(x) = \frac{12 + \lambda^2}{12 + \lambda^2 - 3\lambda^2 x_d(1 - x_d)}\left[\frac{x}{x_d} + \left(1 - \frac{x}{x_d}\right)\frac{H(x - x_d)}{1 - x_d} - \frac{3\lambda^2}{12 + \lambda^2}x(1 - x)\right] \tag{11}$$

Note that as the independent parameter λ^2 tends to zero, (11) reverts to the triangular static deflection

$$\phi_1(x)\big|_{\lambda^2 = 0} = \begin{cases} x/x_d, & 0 \le x \le x_d \\ (1 - x)/(1 - x_d), & x_d \le x \le 1 \end{cases} \tag{12}$$

used by Johnson *et al.* (2002a) to model a taut cable (where $\lambda^2 = 0$). The remaining shape functions are sine functions:

$$\phi_{j+1}(x) = \sin \pi j x, \quad j=1,...,m-1 \tag{13}$$

Substituting the shape functions into the nondimensional equation of motion (1) and simplifying results in the matrix equation

$$\mathbf{M}\ddot{\mathbf{q}} + \mathbf{C}\dot{\mathbf{q}} + \mathbf{K}\mathbf{q} = \mathbf{f} + \boldsymbol{\varphi} F_d(t) \tag{14}$$

with mass $\mathbf{M} = [m_{ij}]$, damping $\mathbf{C} = c\mathbf{M}$, and stiffness $\mathbf{K} = [k_{ij}]$ matrices

$$m_{ij} = \int_0^1 \phi_i(x)\phi_j(x)dx$$

$$= \begin{cases} \frac{1}{2}\delta_{ij}, & i > 1,\ j > 1 \\ \dfrac{48 + \frac{1}{30}\lambda^2[4\lambda^2 + 60 - 15(12 + \lambda^2)x_d(1 - x_d)]}{[12 + \lambda^2 - 3\lambda^2 x_d(1 - x_d)]^2}, & i = 1,\ j = 1 \\ \dfrac{12 + \lambda^2}{12 + \lambda^2 - 3\lambda^2 x_d(1 - x_d)}\left[\dfrac{\sin k\pi x_d}{x_d(1 - x_d)k^2\pi^2}\right], & \text{otherwise, even } k \text{ where } k = \max\{i, j\} - 1 \\ \dfrac{12 + \lambda^2}{12 + \lambda^2 - 3\lambda^2 x_d(1 - x_d)}\left[\dfrac{\sin k\pi x_d}{x_d(1 - x_d)k^2\pi^2} - \dfrac{12\lambda^2}{k^3\pi^3(12 + \lambda^2)}\right], & \text{otherwise, odd } k \text{ where } k = \max\{i, j\} - 1 \end{cases} \tag{15}$$

$$c_{ij} = c\int_0^1 \phi_i(x)\phi_j(x)dx = cm_{ij} \tag{16}$$

§ It can be shown that the peak of $w_{static}(x)$ always occurs at $x = x_d$.

$$k_{ij} = \frac{1}{\pi^2}\left[\lambda^2\left\{\int_0^1 \phi_i(x)dx \int_0^1 \phi_j(x)dx\right\} + \int_0^1 \phi_i'(x)\phi_j'(x)dx\right] = \lambda^2 k_i^{\text{sag}} k_j^{\text{sag}} + k_{ij}^{\text{tension}}$$

$$k_i^{\text{sag}} = \begin{cases} \dfrac{6}{[12+\lambda^2-3\lambda^2 x_{\text{d}}(1-x_{\text{d}})]\pi}, & i = 1 \\ \dfrac{2}{(i-1)\pi^2}, & \text{even } i \\ 0, & \text{otherwise} \end{cases} \tag{17}$$

$$k_{ij}^{\text{tension}} = \begin{cases} \dfrac{1}{2}(i-1)^2\delta_{ij}, & i > 1,\ j > 1 \\ \dfrac{1}{x_{\text{d}}(1-x_{\text{d}})\pi^2} + \dfrac{3\lambda^4(3x_{\text{d}}^2-3x_{\text{d}}+1)}{[12+\lambda^2-3\lambda^2 x_{\text{d}}(1-x_{\text{d}})]^2\pi^2}, & i = 1,\ j = 1 \\ \dfrac{12+\lambda^2}{\pi^2[12+\lambda^2-3\lambda^2 x_{\text{d}}(1-x_{\text{d}})]}\left[\dfrac{\sin k\pi x_{\text{d}}}{x_{\text{d}}(1-x_{\text{d}})}\right], & \text{otherwise, even } k \text{ where } k = \max\{i,j\}-1 \\ \dfrac{12+\lambda^2}{\pi^2[12+\lambda^2-3\lambda^2 x_{\text{d}}(1-x_{\text{d}})]}\left[\dfrac{\sin k\pi x_{\text{d}}}{x_{\text{d}}(1-x_{\text{d}})} - \dfrac{12\lambda^2}{k\pi(12+\lambda^2)}\right], & \text{otherwise, odd } k \text{ where } k = \max\{i,j\}-1 \end{cases}$$

externally applied load vector $\mathbf{f} = [f_1 \quad f_2 \quad \dots \quad f_m]^{\text{T}}$

$$f_i = \int_0^1 f(x,t)\phi_i(x)dx \tag{18}$$

vector $\mathbf{q} = [q_j]$ of generalized displacements, and damper load vector $\boldsymbol{\varphi}$

$$\boldsymbol{\varphi} = \boldsymbol{\phi}(x_{\text{d}}) = [\phi_1(x_{\text{d}}) \quad \phi_2(x_{\text{d}}) \quad \dots \quad \phi_m(x_{\text{d}})]^{\text{T}} = [1 \quad \sin(1\pi x_{\text{d}}) \quad \dots \quad \sin(\{m-1\}\pi x_{\text{d}})]^{\text{T}} \tag{19}$$

Note that the stiffness in (17) is comprised of stiffness due to tension, as in the taut-string model, plus additional stiffness due to sag that only affects the modes not antisymmetric about the center of the cable. Further, note that the mass (15), damping (16), and stiffness (17) elements reduce exactly to the corresponding equations in Johnson *et al.* (2002a) in the absence of sag.

The resulting model captures the salient features of a cable damper system much better than with sine terms alone. With just 11 terms (static deflection plus 10 sine terms), the first several natural frequencies, damping ratios, and mode shapes are more accurate than those computed with 100 sine terms alone. Increasing to 21 terms (static deflection plus 20 sine terms) provides better accuracy than several hundred sine-only terms. Convergence tests showed this to be true in the uncontrolled case, in the case with the optimal passive linear viscous damper, and with an active damper. For the remainder of this study, 21 terms (static deflection plus 20 sine terms) will be employed.

For control design, the system dynamics may be equivalently written in state-space form with input/output relations

$$\begin{aligned} \dot{\boldsymbol{\eta}} &= \mathbf{A}\,\boldsymbol{\eta} + \mathbf{B}\,F_{\mathrm{d}}(t) + \mathbf{G}\,\mathbf{f} \\ \mathbf{y} &= \mathbf{C}_y\boldsymbol{\eta} + \mathbf{D}_y F_{\mathrm{d}}(t) + \mathbf{H}_y\mathbf{f} + \mathbf{v} \end{aligned} \tag{20}$$

where $\boldsymbol{\eta} = [\mathbf{q}^{\mathrm{T}} \quad \dot{\mathbf{q}}^{\mathrm{T}}]^{\mathrm{T}}$ is the state vector, $\mathbf{y} = [w(x_{\mathrm{d}}, t) \quad \dot{w}(x_{\mathrm{d}}, t)]^{\mathrm{T}} + \mathbf{v}$ is a vector of noisy sensor measurements (includes the displacement and acceleration at the damper location), $\mathbf{v}$ is a vector of stochastic sensor noise processes, and

$$\begin{aligned} \mathbf{A} &= \begin{bmatrix} \mathbf{0} & \mathbf{I} \\ -\mathbf{M}^{-1}\mathbf{K} & -\mathbf{M}^{-1}\mathbf{C} \end{bmatrix} \qquad \mathbf{B} = \begin{bmatrix} \mathbf{0} \\ \mathbf{M}^{-1}\boldsymbol{\varphi} \end{bmatrix} \qquad \mathbf{G} = \begin{bmatrix} \mathbf{0} \\ \mathbf{M}^{-1} \end{bmatrix} \\ \mathbf{C}_y &= \begin{bmatrix} \boldsymbol{\varphi}^{\mathrm{T}} & \mathbf{0} \\ -\boldsymbol{\varphi}^{\mathrm{T}}\mathbf{M}^{-1}\mathbf{K} & -\boldsymbol{\varphi}^{\mathrm{T}}\mathbf{M}^{-1}\mathbf{C} \end{bmatrix} \qquad \mathbf{D}_y = \begin{bmatrix} \mathbf{0} \\ \boldsymbol{\varphi}^{\mathrm{T}}\mathbf{M}^{-1}\boldsymbol{\varphi} \end{bmatrix} \qquad \mathbf{H}_y = \begin{bmatrix} \mathbf{0} \\ \boldsymbol{\varphi}^{\mathrm{T}}\mathbf{M}^{-1} \end{bmatrix} \end{aligned} \tag{21}$$

CONTROL OF CABLE VIBRATION

Three types of dampers are considered in this study. The damper of primary interest is a general semiactive device, one that may exert any required *dissipative* force. However, comparison with passive linear viscous dampers, similar to the oil dampers that have been installed in numerous cable-stayed bridges, is vital to demonstrate the improvements that may be gained with semiactive damping technology. Additionally, comparison with active control devices is useful as they bound the achievable performance.

Passive Viscous Damper

If the damping device is a passive linear viscous damper, then the damper force is

$$F_{\mathrm{d}}(t) = -c_{\mathrm{d}}\dot{w}(x_{\mathrm{d}}, t) \tag{22}$$

where c_{d} is a nondimensional damping constant and $\dot{w}(x_{\mathrm{d}}, t)$ is the nondimensional velocity at the damper location

$$\dot{w}(x_{\mathrm{d}}, t) = \sum_{i=1}^{m} \dot{q}_i(t)\phi_i(x_{\mathrm{d}}) = \boldsymbol{\varphi}^{\mathrm{T}}\dot{\mathbf{q}} = [\mathbf{0}^{\mathrm{T}} \quad \boldsymbol{\varphi}^{\mathrm{T}}]\boldsymbol{\eta} \tag{23}$$

The modal damping may be determined via a straightforward eigenvalue analysis. Note that the optimal passive damper supplies pure damping; stiffness tends to degrade the damper performance (Sulekh, 1990; Xu *et al.*, 1998b).

Alternate Measures of Damper Performance

Modal damping ratios provide a useful means of determining the effectiveness of linear viscous damping strategies. However, using a semiactive damper introduces a nonlinearity into the combined system. Consequently, performance measures other than modal damping must be used for judging the efficacy of nonlinear damping strategies in comparison with linear (passive or active) dampers.

Using the root mean square (RMS) or peak response of the cable at some particular location (or several locations) is one possible measure of damper performance. However, it may be possible for one control strategy to decrease the motion significantly in some regions of a structure but allow other parts to vibrate relatively unimpeded. Thus, the primary measure of damper performance considered herein is the mean square cable deflection integrated along the length of the cable, defined by

$$\sigma^2_{\text{displacement}}(t) \;=\; E\left[\int_0^1 w^2(x,t)dx\right] \;=\; E[\mathbf{q}^{\mathrm{T}}(t)\mathbf{M}\mathbf{q}(t)] \;=\; \text{trace}\{\mathbf{M}^{1/2}E[\mathbf{q}(t)\mathbf{q}^{\mathrm{T}}(t)]\mathbf{M}^{1/2}\} \tag{24}$$

where $\mathbf{M}^{1/2}$ is a square symmetric matrix such that $\mathbf{M}^{1/2}\mathbf{M}^{1/2} = \mathbf{M}$. The corresponding RMS cable velocity may be computed from the generalized velocities

$$\sigma^2_{\text{velocity}}(t) \;=\; E[\dot{\mathbf{q}}^{\mathrm{T}}(t)\mathbf{M}\dot{\mathbf{q}}(t)] \;=\; \text{trace}\{\mathbf{M}^{1/2}E[\dot{\mathbf{q}}(t)\dot{\mathbf{q}}^{\mathrm{T}}(t)]\mathbf{M}^{1/2}\} \tag{25}$$

For stationary response to a stationary stochastic excitation, these performance measures become constant and not functions of time.

Active Damper

The optimal passive viscous damper provides one benchmark against which to judge semiactive dampers. The other end of the spectrum of control possibilities is an ideal active damper, which may exert any desired force. The performance of the actively controlled systems give a performance target for semiactive control.

One family of H_2/LQG control designs is considered in this study. This family of controllers performed well for cables without sag (Johnson *et al.*, 2002a). These controllers use force proportional to an estimate of the state of the system, $F_{\text{d}}^{\text{active}}(t) = -\mathbf{L}\hat{\boldsymbol{\eta}}$, where $\mathbf{L} = R^{-1}\mathbf{B}^{\mathrm{T}}\mathbf{P}$ is the feedback gain that minimizes the cost function

$$J \;=\; \tfrac{1}{2}(\sigma^2_{\text{displacement}} + \sigma^2_{\text{velocity}}) + R\sigma^2_{\text{force}} \;=\; \lim_{T\to\infty}\; E\left[\frac{1}{T}\int_0^T (\tfrac{1}{2}\mathbf{q}^{\mathrm{T}}\mathbf{M}\mathbf{q} + \tfrac{1}{2}\dot{\mathbf{q}}^{\mathrm{T}}\mathbf{M}\dot{\mathbf{q}} + RF_{\text{d}}^2)dt\right] \tag{26}$$

where $\mathbf{P}$ satisfies the algebraic Riccati equation

$$\mathbf{A}^{\mathrm{T}}\mathbf{P} + \mathbf{P}\mathbf{A} - \mathbf{P}\mathbf{B}R^{-1}\mathbf{B}^{\mathrm{T}}\mathbf{P} + \mathbf{Q} \;=\; \mathbf{0} \tag{27}$$

with

$$\mathbf{Q} \;=\; \begin{bmatrix} \frac{1}{2}\mathbf{M} & \mathbf{0} \\ \mathbf{0} & \frac{1}{2}\mathbf{M} \end{bmatrix} \tag{28}$$

By varying the control weight R, a family of controllers that use varying force levels can be designed.

A standard Kalman filter observer is used to estimate the states of the system

$$\dot{\hat{\boldsymbol{\eta}}} \;=\; (\mathbf{A} - \mathbf{L}_{\text{KF}}\mathbf{C}_y)\hat{\boldsymbol{\eta}} + \mathbf{L}_{\text{KF}}\mathbf{y} + (\mathbf{B} - \mathbf{L}_{\text{KF}}\mathbf{D}_y)F_{\text{d}}(t) \tag{29}$$

where $\mathbf{L}_{\mathrm{KF}} = (\tilde{\mathbf{P}}\mathbf{C}_y^{\mathrm{T}} + \mathbf{G}\mathbf{Q}_{\mathrm{KF}}\mathbf{H}^{\mathrm{T}})(\mathbf{R}_{\mathrm{KF}} + \mathbf{H}\mathbf{Q}_{\mathrm{KF}}\mathbf{H}^{\mathrm{T}})^{-1}$ is the estimator gain and $\tilde{\mathbf{P}}$ is computed from the Riccati equation

$$\mathbf{A}\tilde{\mathbf{P}} + \tilde{\mathbf{P}}\mathbf{A}^{\mathrm{T}} - (\tilde{\mathbf{P}}\mathbf{C}_y^{\mathrm{T}} + \mathbf{G}\mathbf{Q}_{\mathrm{KF}}\mathbf{H}_y^{\mathrm{T}})(\mathbf{R}_{\mathrm{KF}} + \mathbf{H}\mathbf{Q}_{\mathrm{KF}}\mathbf{H}^{\mathrm{T}})^{-1}(\mathbf{C}_y\tilde{\mathbf{P}} + \mathbf{H}_y\mathbf{Q}_{\mathrm{KF}}\mathbf{G}^{\mathrm{T}}) = -\mathbf{G}\mathbf{Q}_{\mathrm{KF}}\mathbf{G}^{\mathrm{T}} \qquad (30)$$

where $\mathbf{Q}_{\mathrm{KF}}$ is the magnitude of the excitation spectral density $\mathbf{S}_{\mathbf{ff}}(\omega)$, $\mathbf{R}_{\mathrm{KF}}$ the magnitude of noise spectral density $\mathbf{S}_{\mathbf{vv}}(\omega)$, $E[\mathbf{f}] = \mathbf{0}$, $E[\mathbf{v}] = \mathbf{0}$, where $E[\cdot]$ is the expectation operator, and excitation $\mathbf{f}$ and sensor noise $\mathbf{v}$ are uncorrelated.

Semiactive Damper

Unlike an active device, a semiactive damper, such as a variable-orifice viscous damper, a controllable friction damper, or a controllable fluid damper (Spencer and Sain, 1997; Housner *et al.*, 1997), can only exert *dissipative* forces. Herein, a generic semiactive device model is assumed that is purely dissipative. Essentially, this requirement dictates that the force exerted by the damper and the velocity across the damper must be of opposite sign; *i.e.*, $F_{\mathrm{d}}(t)\dot{w}(x_{\mathrm{d}}, t)$ must be less than zero. Figure 3 shows this constraint graphically (the vertical axis is the negative of the force since positive force and positive velocity are here assumed in the same, not opposite, directions). A clipped optimal strategy is used, with a primary controller based on the same family of H_2/LQG designs used for the active damper, and a secondary controller to account for the nonlinear nature of the semiactive device

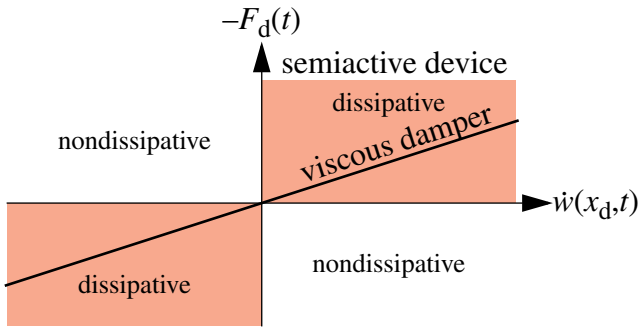

Figure 3. Semiactive damper dissipative forces.

$$F_{\mathrm{d}}(t) = \begin{cases} F_{\mathrm{d}}^{\mathrm{active}}(t), & F_{\mathrm{d}}^{\mathrm{active}}(t)\dot{v}(x_{\mathrm{d}}, t) < 0 \\ 0, & \text{otherwise} \end{cases} \qquad (31)$$

Here, the secondary controller simply clips non-dissipative commands. For implementation in experiment or full-scale application, a bang-bang controller with force feedback has been shown to be effective (Dyke, 1996).

EFFICACY OF SMART DAMPING STRATEGIES

The phenomena that cause rain-wind induced vibration, including the aerodynamic forces, motion of water rivulets, the nonlinear coupling with the cable motion, and so forth, are not well understood (Main and Jones, 1999); consequently, there are no well established models of this behavior. However, it has been observed that the response tends to be dominated by the first several modes (Yoshimura *et al.*, 1988; Main and Jones, 2001). In the absence of a suitable model, the cable/damper system is here simulated with a stationary Gaussian white noise excitation shaped by the first mode of the cable with no sag (*i.e.*, a half-sine). Without a supplemental damper, and in the absence of sag, this half-sine excitation would energize just the first mode of the cable. A range of damper locations and λ^2 are studied herein. The cable is assumed to have virtually no inherent damping without the supplemental damper: $c = 0.0001$ which corresponds to 0.005% in the first mode. A non-zero damping is used so that the RMS responses of the cable approach a finite value, and not infinity, as control effort is decreased. The level of damping should not be interpreted to imply an actual level of damping in the cable, which may be a function of the level of sag and amplitude of vibration (Yamaguchi and Adhikari, 1995), but merely an observation that generally

very low inherent damping is present in stay cables. RMS responses to the excitation are computed via a Lyapunov solution for linear (passive and active) strategies and from simulation for semiactive dampers. A 1% RMS sensor noise corrupts each sensor measurement (modelled as Gaussian pulse processes).

Damping Ratio for Linear Control Strategies

The interest herein is primarily on the RMS cable responses with semiactive dampers. However, some insight can be gained by looking first at the modal properties of the controlled system. Since the semiactive system is, by definition, nonlinear, the active system with state feedback will be used to compute modal properties and will be compared with passive modal damping. The RMS responses of the optimal output-feedback active and the best semiactive damping strategies will be seen below to be quite similar. Thus, the modal properties of the active system are good indicators of "equivalent" modal properties for the semiactive system. Previous studies (*e.g.*, Sulekh, 1990; Xu *et al.*, 1998a) have shown that the primary effects of sag on the efficacy of transverse passive dampers are in the first symmetric mode. Here, the properties of the first symmetric and first antisymmetric modes are examined for various levels of λ^2. Higher modes tend to follow trends similar to the first antisymmetric mode as λ^2 increases.

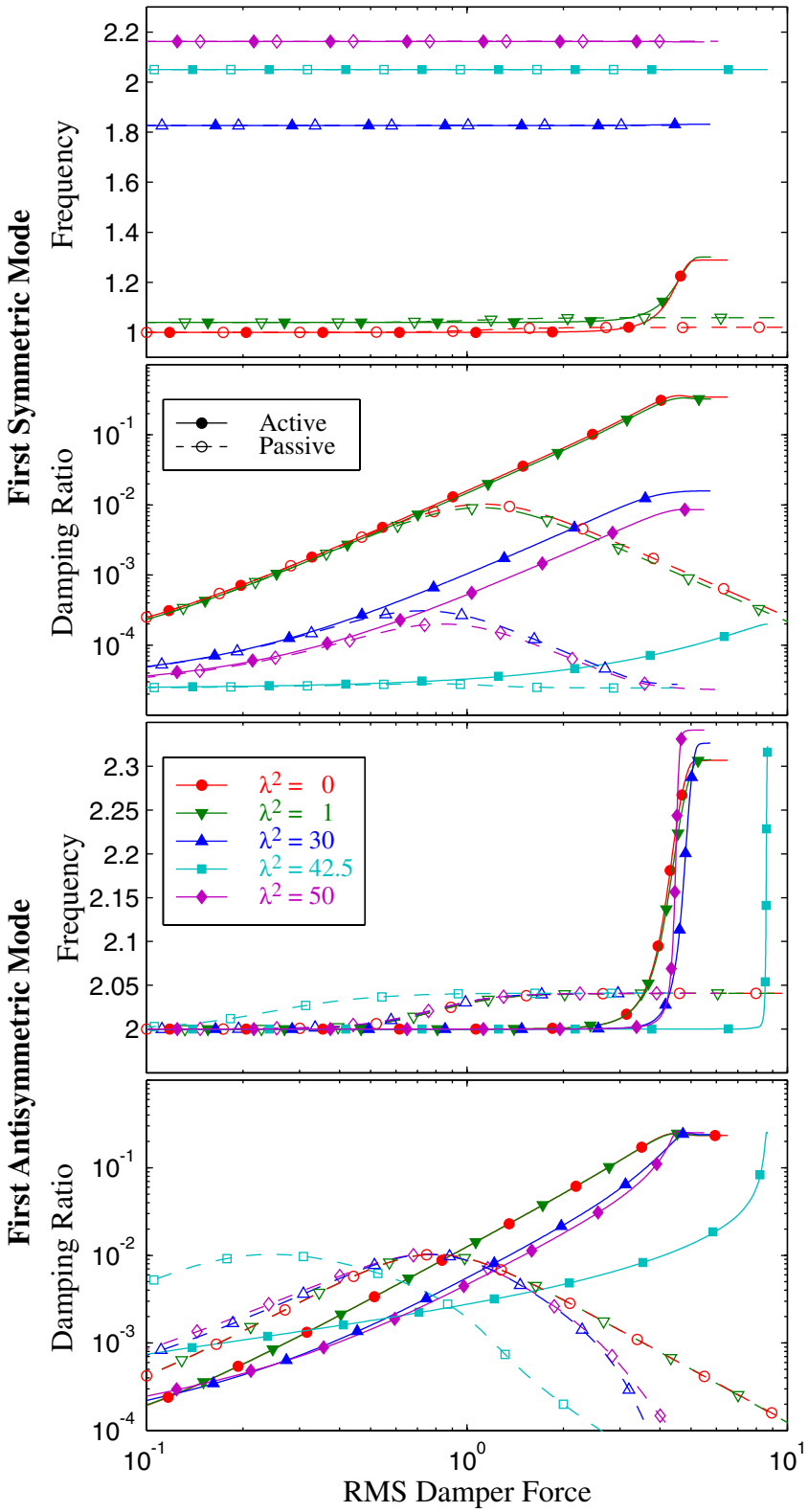

Figure 4. Natural frequency and damping ratio in the first two modes for the linear designs for $x_d = 0.02$.

The modal damping that can be provided to the first two modes of the cable/damper system by passive and active dampers is shown in Figure 4 for a damper location $x_d = 0.02$. (The reader may note that the five markers, whether filled or not, denote different levels of λ^2, whereas dashed lines with open markers

denote the passive results, and solid lines with filled markers denote the active results.) The various control strategies are based on varying the passive damper coefficient c_d or the active control weight R. (Note: extremely aggressive active controllers — *i.e.*, those with very large forces — are not shown in Figure 4; they underperform relative to moderately aggressive controllers, both for active controllers for most levels of λ^2 as well as when used as part of a clipped-optimal strategy for semiactive dampers.) In the absence of sag, the maximum damping in the first symmetric mode provided by a passive damper is 1.03%, whereas the active damper provides over 36% of critical damping. With small sag, $\lambda^2 = 1$, the passive damping is degraded slightly to 0.91% (a factor of 0.88); the active system drops to 33.6% (a factor of 0.93). For a larger sag $\lambda^2 = 30$, the passive damper is less effective, providing only 0.04% damping (a factor of 0.039 compared to no sag). The active device, however, still provides almost a 1.6% damping ratio (a factor of 0.044 compared to no sag). For $\lambda^2 = 42.5$, the passive damper is ineffective for the first symmetric mode, providing only 0.002% damping. The active device for this particular level of sag is also severely reduced, providing only 0.04% damping. For yet larger sag at $\lambda^2 = 50$, a passive damper can provide 0.04% damping and the active strategy can provide 1% damping in the first symmetric mode. The natural frequency of the first symmetric mode for larger sag increases to over twice the value at small sag. The natural frequencies remain relatively constant over the range of x_d.

Sag has virtually no effect on the magnitude of optimal passive damping ratio for the first antisymmetric mode; this is consistent with previous studies (Sulekh, 1990), with the damping remaining about 1% of critical. Similarly, the peak modal damping in the first antisymmetric mode provided by the active control is unaffected by the inclusion of sag, achieving 30% damping. Higher symmetric and antisymmetric modes follow similar trends. Figure 4 does indicate that an optimal level of control does exists for both the passive control (as seen in previous studies with optimal damper sizes) and for the active control strategy. In general, the optimal passive or active damping force for the first symmetric and first antisymmetric modes are similar in magnitude but not identical. However, it should be noted, the optimal passive damping force for $\lambda^2 = 42.5$ is significantly smaller for maximizing the damping of the first antisymmetric mode than that of the first symmetric mode. This would indicate that, for levels of sag near this range, one must choose between designing for optimal damping in the first symmetric or first antisymmetric mode. This is not the case for active control.

The passive results computed here are comparable to those in previous studies, thus further verifying the control-oriented model used herein. Table 1 shows a comparison of the peak modal damping ratio that can be achieved with a passive damper for several sag levels, comparing to the results of Sulekh (1990) and Xu *et al.* (1998a) for $x_d = 0.02$. The former used a Galerkin approach, requiring 350 sine shape functions, whereas the latter used a hybrid method they developed, requiring 400 degrees-of-freedom. Comparing the results of these two previous studies to those found in this study, it is clear that the design oriented model used here is both efficient, requiring only 21 degrees-of-freedom, and accurate, resulting in damping values bounded by the two previous studies.

Table 1. Comparison of peak modal damping ratios with a linear passive viscous damper at $x_d = 0.02$.

λ^2	*mode*	*Sulekh (1990)*	*Xu et al. (1998a)*	*this study*
$\lambda^2 = 0$	first (symmetric)	1.10%	—	1.03%
$\lambda^2 = 0.245$	first (symmetric)	—	0.98%	1.00%
$\lambda^2 = 1$	first (symmetric)	0.95%	—	0.91%
$\lambda^2 = 1.20$	first (symmetric)	—	0.85%	0.89%
$\lambda^2 = 3.63$	first (symmetric)	—	0.64%	0.68%
	others	1.10%	1.04%	1.03%

The effects of sag and inclination on modal characteristics of the controlled system, in particular on the first symmetric and first antisymmetric modes of vibration, may be better seen in Fig. 5. Here, for each value of λ^2, the passive and active strategies used are those that give maximal damping in the first symmetric mode. As λ^2 approaches 40, the passive control of both first symmetric and first antisymmetric modes is significantly reduced — indeed, it is ineffective at $\lambda^2 = 4\pi^2 = 39.478$ and at $\lambda^2 = 41.93$. The reduced effects of passive damping on the first antisymmetric mode damping ratio results from the fact that the "optimal" passive damper is defined with respect to the damping ratio of the first symmetric mode and, over this range of λ^2, the optimal passive first symmetric and first antisymmetric systems occur at different levels of damper force. Reasons for these regions of decreased performance for the symmetric modes are discussed in the next section. The symmetric mode is more greatly affected in regions nearby $\lambda^2 = 4\pi^2$ than the first antisymmetric mode. The active control damping is similarly affected, although the active strategy is capable of providing significantly increased performance in general. Crossing of the controlled natural frequencies does occur at certain levels of λ^2. It is observed that, for levels of sag below $\lambda^2 = 4\pi^2$, the increase in sag results in a significant decrease in damping in the first symmetric mode for both passive and active control strategies. Increasing the sag beyond $\lambda^2 = 42$ increases the damping in these two modes, eventually to values near that of the taut cable. Both control strategies result in increased natural frequencies as the sag is increased. (Note that higher modes follow the same trends as the first antisymmetric mode.)

Figures 6 and 7 show the frequency and damping ratio of the first symmetric and antisymmetric modes, respectively, over a range of damper locations and for several levels of the independent parameter λ^2. The symmetric mode is affected by sag, particularly for certain combinations of λ^2 and damper location. For example, $\lambda^2 = 42.5$ drops to minimal damping near $x_d = 0.025$ for both passive and active strategies. The antisymmetric mode is somewhat different; active control is quite effective in adding damping to this mode over a wide range of sag and damper location. The passive has some areas where it does not perform well.

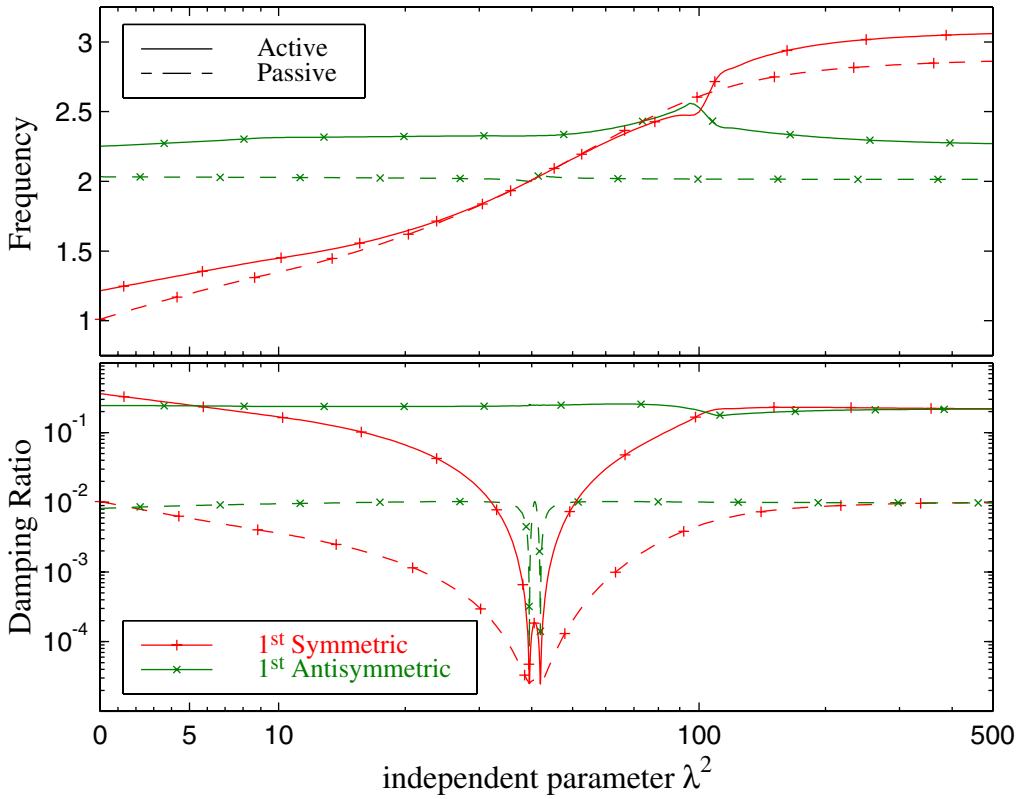

Figure 5. Modal frequency and damping ratios over a range of sag with a damper at $x_d = 0.02$.

RMS Cable Response

The RMS cable displacement, defined in (24), as well as the RMS cable velocity and RMS damper force, were computed using a Lyapunov solution for passive and active (output feedback) control strategies, but through simulation for the semiactive system. Due to minimal damping in less aggressive control strategies, and the very long simulation times required to accurately determine RMS responses, only several semiactive controllers in the family of possible controllers are simulated here. (As a result, the improvements shown herein for an ideal semiactive damper compared to optimal passive linear dampers should be considered conservative.) The responses with the smart damper are shown using large bold markers (the same markers as the active and passive for a given value of the independent parameter λ^2).

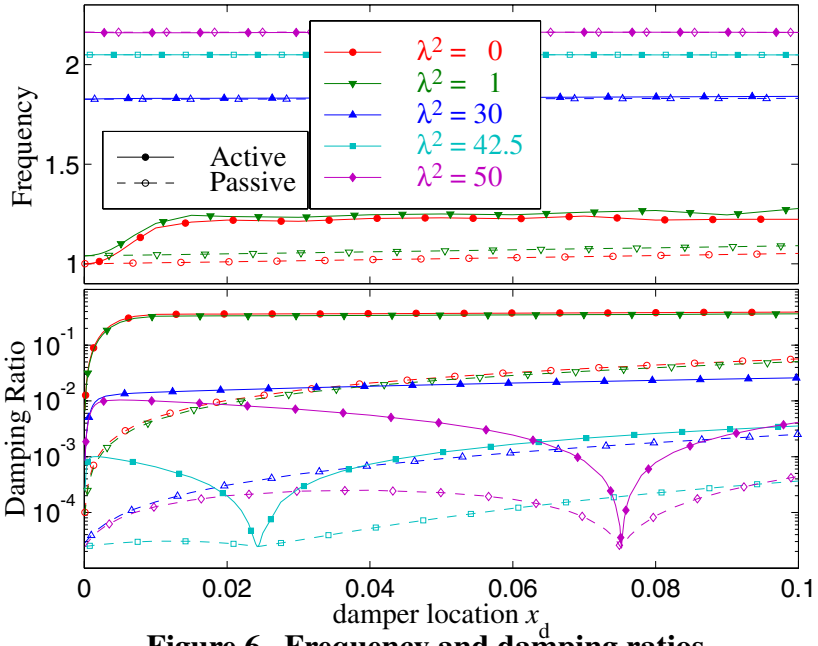

Figure 6. Frequency and damping ratios of first symmetric mode as a function of damper location x_d for several sag levels.

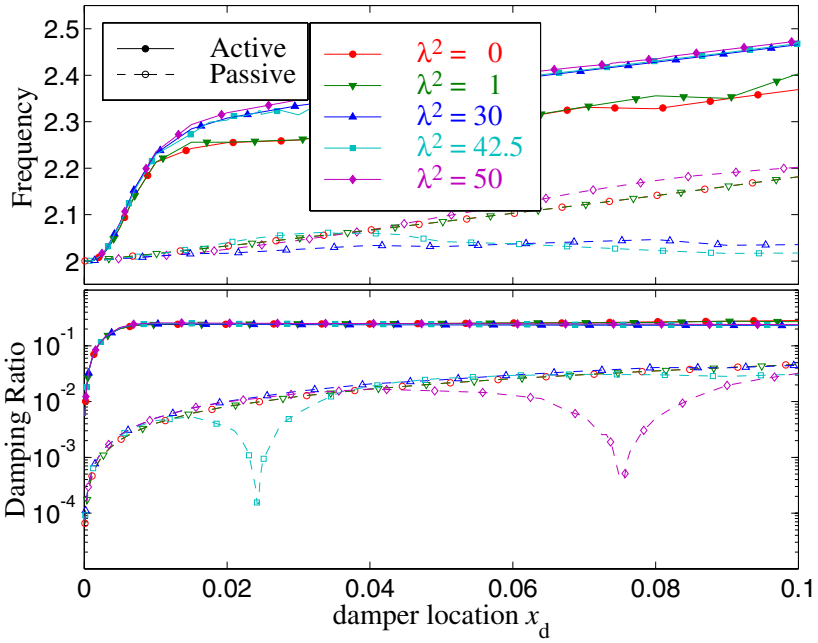

Figure 7. Frequency and damping ratios of first antisymmetric mode as a function of damper location x_d for several sag levels.

Figure 8 shows the RMS cable displacement as a function of the RMS damper force for a damper at $x_d = 0.02$ at several levels of sag. For strategies using small forces, the passive and active are nearly the same — this was also seen in Johnson *et al.* (2002a) where a similar observation may be made about the semiactive strategy as well. However, at some point the passive damper begins to have diminished gains in spite of larger damper forces. This is due to the damper only "knowing" local information, that is, the cable velocity at the damper location. Effectively, the passive damper starts to lock the cable down at that point — certainly limiting the cable motion at the damper location — but allowing the rest of the cable to vibrate nearly unimpeded. The active and semiactive strategies, however, are able to take advantage of larger force levels in such a way that they do not lock the cable down, but rather continue to dissipate energy. The effect is that the controllable smart damper is able to achieve a 50 to 90 percent displacement reduction, depending on the sag, compared to the optimal passive linear viscous damper.

Figure 9 shows the RMS cable displacement for the passive linear viscous damper, the optimal active damper, and the best semiactive damper versus the independent parameter λ^2. Without sag ($\lambda^2 = 0$), the semiactive damper can provide about a 71% response decrease compared to the best passive device. With small sag ($\lambda^2 = 1$), the RMS displacements decrease minutely for all three damping strategies. For $\lambda^2 = 30$ the control performance for passive, active, and semiactive strategies begin to degrade and around $\lambda^2 = 40$, the same region where the damping in the first two modes was significantly decreased, the RMS performance is poor. Increasing λ^2, the performance improves, but there are additional regions where all methods are ineffective. This phenomenon will be discussed in detail in the next section. Nevertheless, the semiactive damper always decreases response compared to the best passive damper, by 60 to 80 percent in most regions.

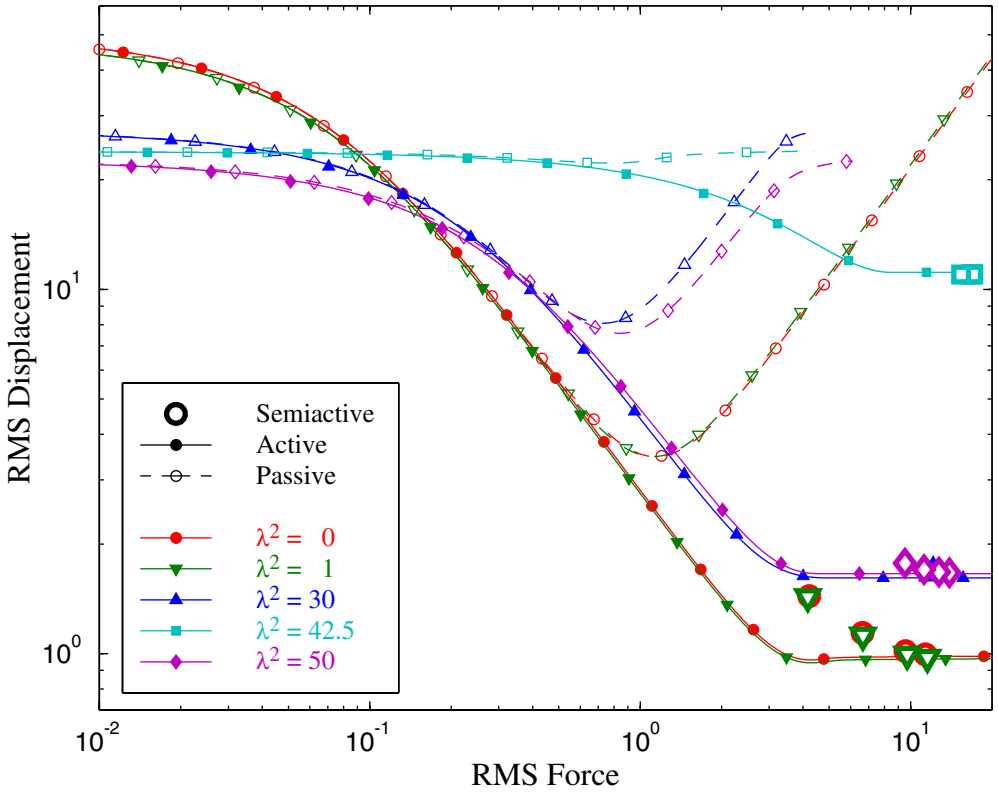

Figure 8. RMS displacement for a semiactive, passive viscous, or active dampers at $x_d = 0.02$ as a function of the RMS force.

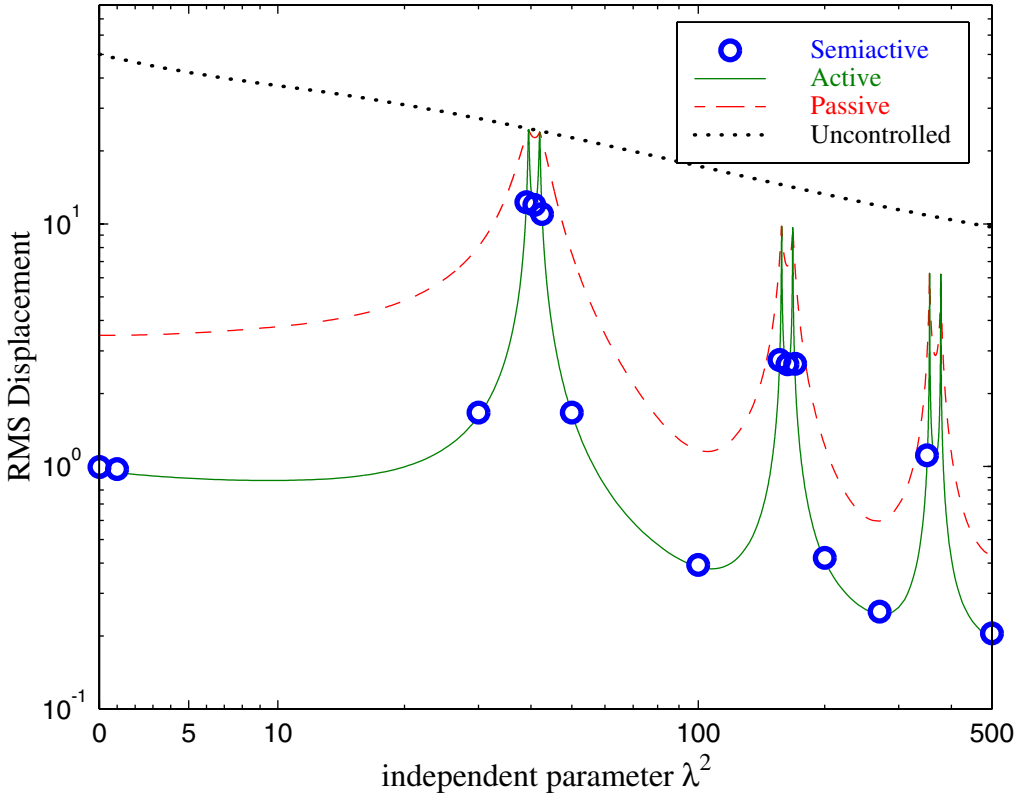

Figure 9. Minimum RMS displacement for a semiactive, passive viscous, or active dampers at $x_d = 0.02$.

To observe what happens near the peaks of reduced performance, Fig. 10 provides a closer look. Indeed, the region of decreased performance around $\lambda^2 = 40$ consists of two peaks of lousy performance with a valley of mediocre performance. The pairing of these two peaks is found for each of the three regions of decreased performance in the [0,500] range of λ^2 values studied here. The peaks of poor performance occur at λ^2 values of $4\pi^2$, 41.93, $16\pi^2$, 167.79, $36\pi^2$ and 377.59. Similar results may be seen in RMS cable velocity (Johnson *et al.*, 2002b). Thus, it may be concluded that a "smart" damper may provide superior damping to cables for a large range of cable sag. Note, however, that the benefit comes with larger damper forces, though these force levels (Johnson *et al.*, 2001,2002a) are still well within the capabilities of current damper technology.

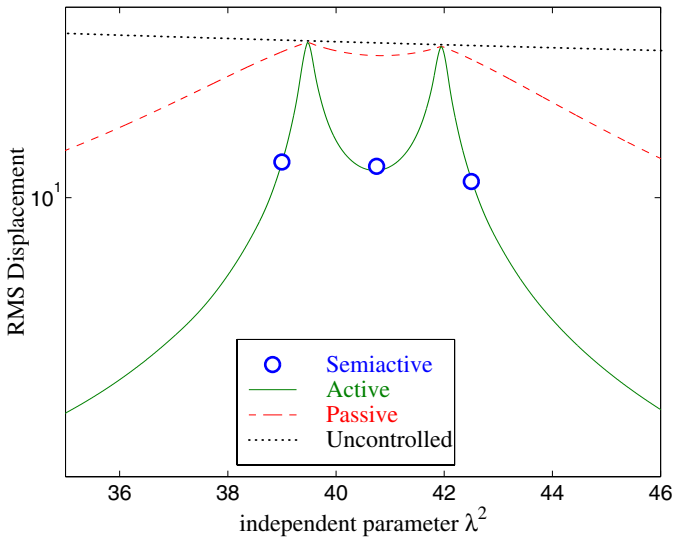

Figure 10. Minimum RMS displacement expanded views near first pair of peaks ($x_d = 0.02$).

Performance at Various Damper Locations

Previous studies with zero sag indicated that, as the damper location approached the support end, semiactive control strategies provided increased performance over the optimal passive strategies. Figure 11 shows the RMS displacement of semiactive, active and passive control strategies for various damper locations and for various level of sag. What is again observed here is that, even for damper locations very near the cable support, semiactive control can provide increased performance for various levels of sag. There are some damper location and sag levels, *i.e.*, some combinations of (x_d,λ^2), that give poor performance for all three vibration mitigation strategies, such as for $\lambda^2 = 42.5$ and 50 near $x_d = 0.025$ and 0.075, respectively (these combinations are discussed in the next section). Even so, the

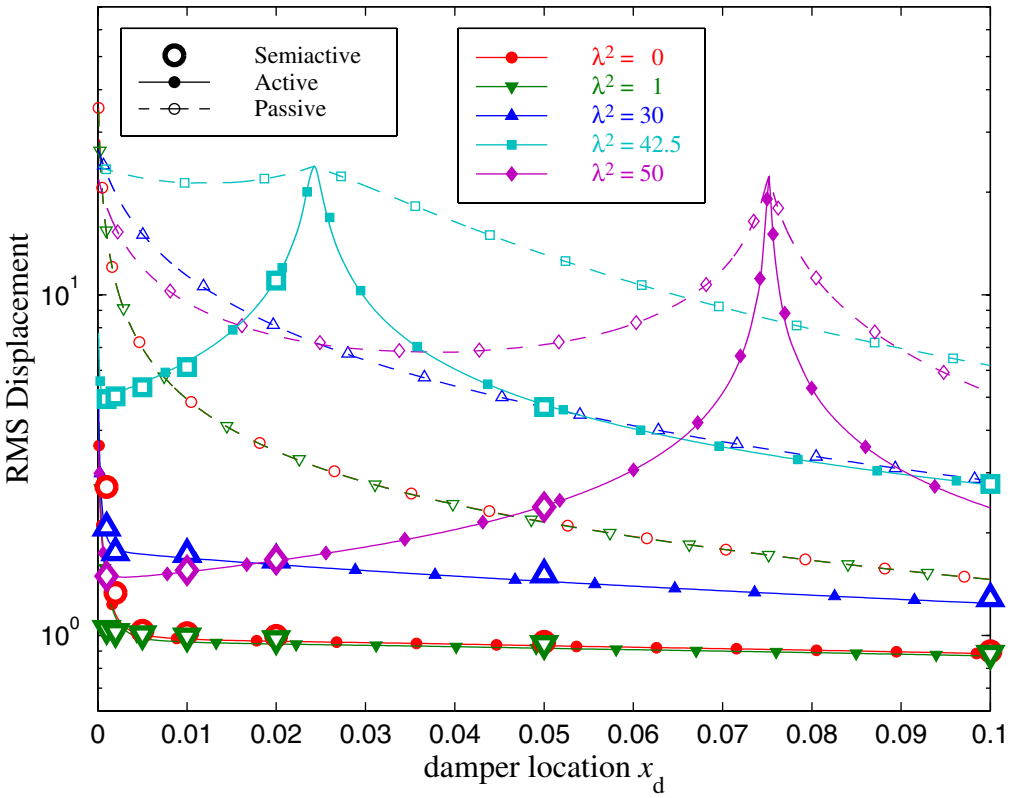

Figure 11. RMS displacement with a semiactive, passive viscous, or active damper at various damper locations.

best semiactive damper always outperforms the passive, usually by a wide margin. Similar trends may also be observed for RMS velocity (Johnson *et al.*, 2002b). To better highlight the relative improvements of a semiactive damper compared to the optimal passive linear viscous damper, Fig. 12 shows the RMS displacement, relative to that of the optimal passive linear viscous damper, of the active and semiactive strategies for several sag levels and over a range of damper locations. For damper locations around $x_d = 0.05$, the response with a semiactive damper is 55% to 70% less than with the passive damper. For most levels of sag, the superior relative performance only gets better for a damper closer to the end of the cable (except when it is *very* close to the end of the cable).

To better see the superior performance of semiactive dampers for this application, Table 2 lists the RMS cable displacements and RMS damper forces, for the optimal linear passive damper and for the best semiactive damper, at several levels of λ^2 and damper location x_d. (It should be noted that due to the computational intensity of the simulations, only a limited number of control weights R were simulated for the semiactive system in each key value of λ^2 and x_d; consequently, the semiactive results are conservative in that even better performance may be available by fine-tuning the control strategy.) The ratios between passive and semiactive strategies are shown in Table 3. Here, the *displacement ratio* is the RMS cable displacement with the optimal passive damper divided by that of the best semiactive damper studied herein. The *force ratio* is the RMS cable displacement with the best semiactive damper divided by that of the optimal passive damper. RMS response using a semiactive damper 2 to 3 times lower than the optimal linear passive damper at damper location $x_d = 0.05$ for levels of sag typical in bridge stay cables. This superior performance increases as the damper location is moved closer to the end of the cable: 5 or 6 times lower response at $x_d = 0.01$ and 12–14 times smaller at $x_d = 0.001$. These improvements over the passive system come at the price of large force levels. However, these larger forces are still well within the cost-effective range of existing semiactive damping devices (Baker, 1999; Johnson *et al.*, 2001,2002a). Further, less aggressive semiactive strategies may be used if the force levels are considered too large, with some reduction in the performance improvement compared to passive strategies.

Table 2. RMS displacements and forces with semiactive and optimal passive control strategies.†

	$\lambda^2 = 0$				$\lambda^2 = 1$				$\lambda^2 = 30$				$\lambda^2 = 42.5$			
	displ.		*force*		*displ.*		*force*		*displ.*		*force*		*displ.*		*force*	
x_d	*P*	*SA*	*P*	*SA*	*P*	*SA*	*P*	*SA*	*P*	*SA*	*P*	*SA*	*P*	*SA*	*P*	*SA*
0.001	15.07	1.07	4.77	200.08	15.03	1.05	4.75	206.21	22.69	1.79	2.04	203.09	23.34	4.94	1.06	200.76
0.002	10.90	1.05	3.45	104.58	10.89	1.02	3.44	107.32	19.85	1.75	1.78	102.10	22.92	5.03	0.88	93.02
0.010	4.94	1.02	1.57	19.85	4.94	0.99	1.57	19.48	11.37	1.73	1.05	16.72	21.28	6.13	0.70	20.70
0.020	3.48	1.00	1.12	11.35	3.47	0.98	1.12	11.53	8.08	1.67	0.70	12.11	22.21	11.00	0.78	16.23
0.050	2.16	0.96	0.71	7.20	2.15	0.94	0.71	7.51	4.68	1.56	0.41	7.87	13.15	4.68	0.39	7.14
0.100	1.46	0.90	0.55	5.17	1.46	0.88	0.55	5.07	2.84	1.31	0.27	4.40	6.20	2.79	0.21	7.87

† *P* = optimal passive, *SA* = best semiactive strategy in this study

Table 3. Relative displacement and forces with semiactive and optimal passive control strategies.‡

	$\lambda^2 = 0$		$\lambda^2 = 1$		$\lambda^2 = 30$		$\lambda^2 = 42.5$	
x_d	*displ. ratio*	*force ratio*	*displ. ratio*	*force ratio*	*displ. ratio*	*force ratio*	*displ. ratio*	*force ratio*
0.001	14.0	42.0	14.4	43.4	12.7	100.0	4.7	190.2
0.002	10.4	30.3	10.6	31.2	11.3	57.4	4.6	105.7
0.010	4.9	12.6	5.0	12.4	6.6	15.9	3.5	29.8
0.020	3.5	10.2	3.6	10.3	4.8	17.2	2.0	20.8
0.050	2.3	10.2	2.3	10.6	3.0	19.1	2.8	18.2
0.100	1.6	9.3	1.7	9.1	2.2	16.6	2.2	37.6

‡ *Displacement ratio* = $\sigma^{\text{passive}}_{\text{displacement}} / \sigma^{\text{semiactive}}_{\text{displacement}}$, *Force ratio* = $\sigma^{\text{semiactive}}_{\text{force}} / \sigma^{\text{passive}}_{\text{force}}$

While there are regions of λ^2 and x_d that limit the performance of semiactive dampers (discussed further in the following section), in most cases, they perform significantly better than passive linear viscous dampers. This is true particularly for damper locations close to the end of the cable. The primary reason for this significant improvement is in the nature of the "information" available to the control strategy. For passive dampers, the only information the damper "knows" — *i.e.*, the responses from which damper force are determined — is the velocity of the cable at the damper attachment location. This *local* response is the only information available to the passive damper. Active and semiactive strategies, however, can use observers to estimate the entire state of the cable based on limited measurements. Herein, the measurements are the displacement and acceleration at the damper location. Using knowledge of the cable/damper system dynamics, the observer is able to estimate the displacement and velocity profiles of the cable at any one instant in time, *i.e.*, *global* response information. This is important because the semiactive damping system is able to use larger forces without completely locking down the cable at the damper attachment location.

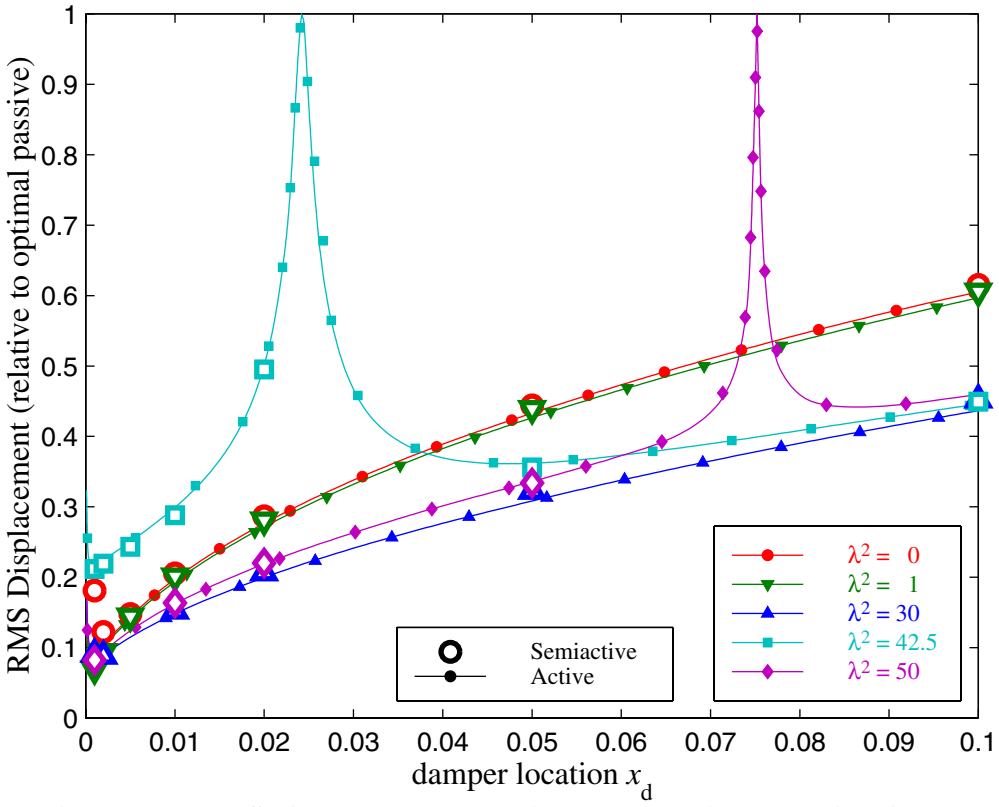

Figure 12. RMS displacement, relative to the optimal passive linear damper, with an active or semiactive damper at various damper locations.

DISCUSSION OF REGIONS OF LIMITED PERFORMANCE

The (x_d,λ^2) regions of poor performance by all three damping strategies (passive, active, and semiactive) are based on specific changes in the underlying dynamics of the cable alone. These changes are explored here to explain the performance results shown in the previous section, both in terms of modal properties and RMS response.

In the absence of a supplemental damper, the mode shapes of the cable without sag ($\lambda^2 = 0$) are sine functions, with integer natural frequencies. However, as the independent parameter λ^2 increases, the mode shapes that are symmetric about the center of the cable change significantly, while the antisymmetric mode shapes remain the same. These effects are discussed in depth elsewhere (*e.g.*, Irvine, 1981), but as these changes ultimately affect the performance of a damper, some details are given here to explain the variations in damper performance that was seen above.

Figure 13 shows the first six natural frequencies of a sag cable as a function of the independent parameter λ^2. Note particularly that due to the increased stiffness on the symmetric modes, there are a number of frequency crossover points, where two modes have identical natural frequencies. These crossovers occur at $\lambda^2 = 4\pi^2$, $16\pi^2$, $36\pi^2$, etc. — *i.e.*, at $\lambda^2 = (2i\pi)^2$, $i = 1, 2, 3, \ldots$ (Irvine, 1981). At these points, passive, active, and semiactive damper difficulties may be expected, since the manifold defined by the two modes with identical frequency can have controllable and uncontrollable subspaces with respect to a single point-located damping device. Indeed, the addition of any damping force will cause the motion of the cable to shift such that a node will occur at the damper location, with no possibility of adding damping to that mode.

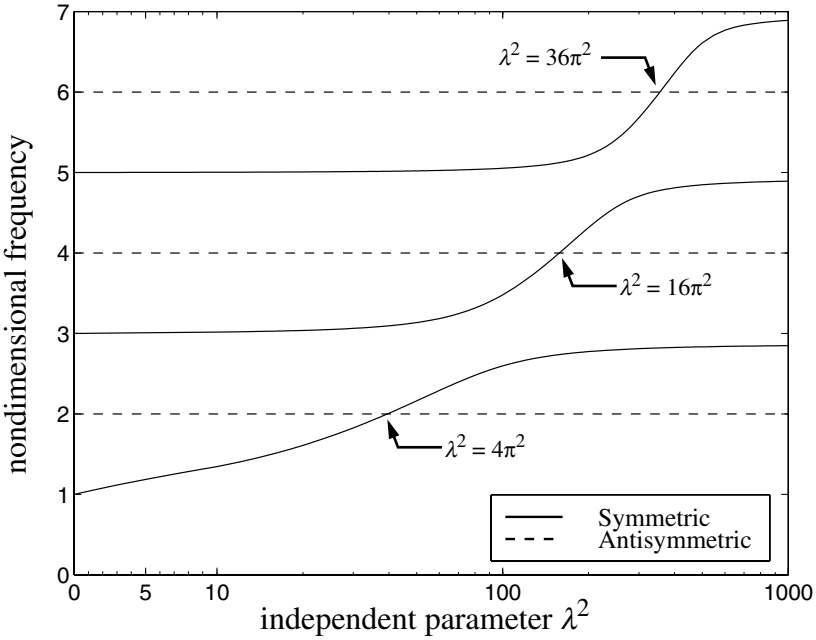

Figure 13. Natural frequencies as a function of the independent parameter λ^2 for sag cables (Irvine, 1981).

Further conditions that may give rise to poor damper performance are when a mode has a node at the damper location. Without sag, this will only occur for rational x_d and only for mode m if an integer i exists such that $i = x_d m$; for small x_d, this will only occur for higher frequency modes. However, with sag, it is possible for the first several symmetric modes to have a node at a typical damper location. Consider the shape of the first symmetric mode[◊] of a flat sag cable, shown for several λ^2 in Fig. 14. At small λ^2, the first symmetric mode is sinusoidal in shape, but the slope at the ends flattens out with increasing sag. At $\lambda^2 = 4\pi^2$, the end slope is zero, as may be seen in Fig. 14. As λ^2 increases beyond $4\pi^2$, the first symmetric mode has a node near each end of the cable. When λ^2 reaches 41.93, the node is at $x = 0.02$;

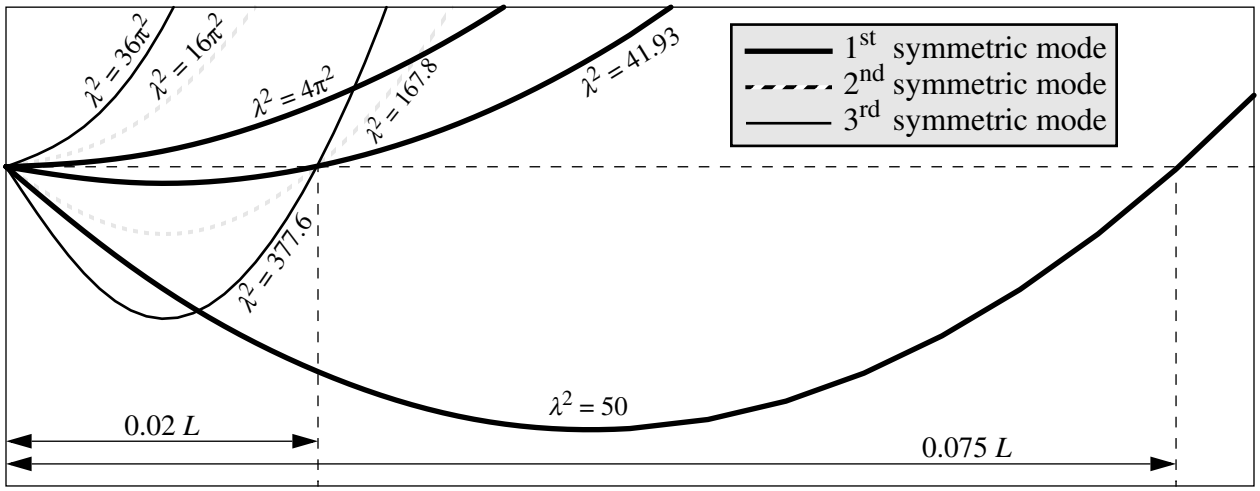

Figure 14. Expanded view of cable modeshapes.

◊ An animation of the effects of sag on cable modeshapes is at http://rcf.usc.edu/~johnsone/animations/cable_sag/

a damper placed at $x_d = 0.02$ would be unable to control the first mode in this case. Similarly, a damper at $x_d \approx 0.025$ and 0.075 could not control the first symmetric mode of a cable with $\lambda^2 \approx 42.5$ and 50, respectively. Nodes will occur near the end of the cable in the second and third symmetric modes for $\lambda^2 > 16\pi^2$ and $\lambda^2 > 36\pi^2$, respectively, causing the second of each pair of response peaks in Fig. 9.

It may be noted that Xu *et al.* (1998a) identify the cause of decreased performance for inclined sag cables, compared to horizontal sag cables, to be related to whether a frequency veering (*e.g.*, Ginsberg and Pham, 1995; Wei and Pierre, 1988) occurs or frequency crossover occurs; however their analysis did not include λ^2 values in the region where the veering vs. crossover has any significant effect (Triantafyllou, 1984). Nevertheless, if the flat-sag parabolic assumption used herein is relaxed to encompass a wider range of sag and inclination, results similar to what was reported above would be expected. Instead of a particular λ^2 where a partially uncontrollable manifold exists, one of the hybrid modes would have a node. Based on the mode shapes given by Triantafyllou (1984), the uncontrollable twin peaks would tend to spread somewhat, but by a small amount for damper locations close to the end of the cable.

CONCLUSIONS

This paper extends a previous study by the authors on ideal "smart" semiactive damping of stay cables. The previous study (Johnson *et al.*, 2002a) showed that significant response reductions are available using semiactive dampers compared to the passive dampers currently in use for mitigating stay cable vibration. Herein, the effects of cable sag, inclination, and longitudinal flexibility have been introduced into the dynamic model of transverse in-plane cable vibration. A new low-order control-oriented model was developed to capture the salient dynamics of the cable/damper system. The performance of passive, active, and semiactive damper strategies are all found to degrade for certain combinations of damper location and independent parameter λ^2 that cause a node to occur at the damper location. When such a case occurs, the three damping strategies perform no better than the cable alone. However, for the general case where a node does not occur at the damper location, semiactive dampers provide significantly improved damping compared to the optimal passive viscous damper. Approximately 50 to 90 percent reduction in RMS response can be achieved compared to the optimal passive linear damper. The cost of this improvement is larger force levels — approximately 5 times larger for damper locations around $x_d = 0.05$, and 8–10 times larger for $x_d = 0.02$. For the zero-sag case, Baker (1999) and Johnson *et al.* (2001,2002a) found that the peak force level during rain-wind induced motion of an example stay cable is on the order of 14 kN (3 kips) for a semiactive damper at $x_d = 0.01$. Thus, these larger forces are well within the cost-effective range of semiactive damping devices such as magnetorheological dampers. Consequently, the ideal semiactive dampers used in this study suggest that smart dampers may be an effective replacement for passive viscous damping of cables.

ACKNOWLEDGEMENTS

The authors gratefully acknowledge the support of this research by the National Science Foundation under grant CMS 99-00234 and the LORD Corporation.

REFERENCES

Baker, G.A. (1999). *Modeling and Semiactive Damping of Stay Cables*. Master's Thesis, Department of Civil Engineering and Geological Sciences, University of Notre Dame.

Christenson, R.E. (2001). *Semiactive Control of Civil Structures for Natural Hazard Mitigation: Analytical and Experimental Studies*, Ph.D. dissertation, Dept. of Civil Engineering and Geological Sciences, University of Notre Dame, Notre Dame, Indiana.

Dyke, S.J., B.F. Spencer, Jr., M.K. Sain, and J.D. Carlson (1996). "Modeling and Control of Magnetorheological Dampers for Seismic Response Reduction." *Smart Materials and Struct.*, **5**, 565–575.

Edwards, A.T., and J.M. Boyd (1965). "Bundle-Conductor-Spacer Design Requirements and Development of 'Spacer-Vibration Damper.'" *IEEE Transactions on Power Apparatus and Systems*, **PAS-84**(10), 924–932.

Endo, T., T. Iijima, A. Okukawa, and M. Ito (1991). "The Technical Challenge of a Long Cable-Stayed Bridge — Tatara Bridge." In M. Ito, Y. Fujino, T. Miyata, and N. Narita (eds.), *Cable-stayed Bridges — Recent Developments and their Future*, Elsevier, 417–436.

Gimsing, N.J. (1983). *Cable-Supported Bridges*, John Wiley & Sons, Chichester, England.

Ginsberg, J.H., and H. Pham (1995). "Forced Harmonic Response of a Continuous system Displaying Eigenvalue Veering Phenomena." *Journal of Vibration and Acoustics*, **117**(4), 439-444.

Housner, G.W., L.A. Bergman, T.K. Caughey, A.G. Chassiakos, R.O. Claus, S.F. Masri, R.E. Skelton, T.T. Soong, B.F. Spencer, Jr., and J.T.P. Yao (1997). "Structural Control: Past and Present." *Journal of Engineering Mechanics*, ASCE, **123**(9), 897–971.

Irvine, H.M. (1981). *Cable Structures*, MIT Press, Cambridge, Massachusetts.

Johnson, E.A., B.F. Spencer, Jr., and Y. Fujino (1999). "Semiactive Damping of Stay Cables: A Preliminary Study." *Proceedings of the 17th International Modal Analysis Conference (IMAC XVII)*, Society for Experimental Mechanics, Bethel, Connecticut, 417–423.

Johnson, E.A., G.A. Baker, B.F. Spencer, Jr., and Y. Fujino (2000). "Mitigating Stay Cable Oscillation using Semiactive Damping." *Smart Structures and Materials 2000: Smart Systems for Bridges, Structures, and Highways* (S.C. Liu, ed.), Proceedings of SPIE, **3988**, 207–216.

Johnson, E.A., G.A. Baker, B.F. Spencer, Jr., and Y. Fujino (2001). *Semiactive Damping of Stay Cables Neglecting Sag.* Technical Report No. USC-CE-01-EAJ1, Dept. of Civil and Environmental Engineering, University of Southern California. Available online at http://rcf.usc.edu/~johnsone/papers/smartdamping_tautcable_rpt.html

Johnson, E.A., G.A. Baker, B.F. Spencer, Jr. and Y. Fujino (2002a). "Semiactive Damping of Stay Cables." *Journal of Engineering Mechanics*, ASCE, **128**(7), in press. Web version online at http://rcf.usc.edu/~johnsone/papers/smartdamping_tautcable_jem.html

E.A. Johnson, R.E. Christenson, and B.F. Spencer, Jr. (2002b). *Flat-Sag Cables with Semiactive Damping.* Technical Report No. USC-CE-02-EAJ1, Dept. of Civil and Environmental Engineering, University of Southern California. Available online at http://rcf.usc.edu/~johnsone/papers/smartdamping_sagcable_rpt.html

Kovacs, I. (1982). "Zur Frage der Seilschwingungen und der Seildampfung." *Die Bautechnik*, **10**, 325–332, (in German).

Krenk, S. (2000). "Vibrations of a Taut Cable with an External Damper." *Journal of Applied Mechanics*, ASME, **67**, 772–776.

Krenk, S., and S.R.K. Nielsen (2002). "Vibrations of Shallow Cable with Viscous Damper." *Proceedings of the Royal Society, Series A: Mathematical, Physical and Engineering Sciences*, London, in press.

Main, J.A., and N.P. Jones (1999). "Full-Scale Measurements of Stay Cable Vibration." In Larsen, Larose, and Livesey (eds.), *Wind Engineering into the 21st Century*, Balkema, Rotterdam, 963–970.

Main, J.A., and N.P. Jones (2001). "Evaluation of Viscous Dampers for Stay-Cable Vibration Mitigation." *Journal of Bridge Engineering*, **6**(6), 385–397.

Pacheco, B.M., Y. Fujino, and A. Sulekh (1993). "Estimation Curve for Modal Damping in Stay Cables with Viscous Damper." *Journal of Structural Engineering*, ASCE, **119**(6), 1961–1979.

Russell, H. (1999). "Hong Kong Bids for Cable-Stayed Bridge Record." *Bridge Design and Engineering*, No. 15 (second quarter), 7.

Spencer, B.F., Jr. and M.K. Sain (1997). "Controlling Buildings: A New Frontier in Feedback." *IEEE Control Systems Magazine*, **17**(6), 19–35.

Stockbridge, G.H. (1925). "Overcoming Vibration in Transmission Cables," *Elec. World*, **86**(26), 1304–1306.

Sulekh, A. (1990). *Non-dimensionalized Curves for Modal Damping in Stay Cables with Viscous Dampers*, Master's Thesis, Department of Civil Engineering, University of Tokyo, Tokyo, Japan.

Triantafyllou, M.S. (1984). "The Dynamics of Taut Inclined Cables." *Journal of Mechanics and Applied Mathematics*, **37**(3), 422–440.

Tunstall, M.J. (1997). "Wind-Induced Vibrations of Overhead Transmission Lines: An Overview." *Proceedings of the International Seminar on Cable Dynamics*, Tokyo, Japan, October 13, 1997, 13–26.

Virloguex, M., *et al.* (1994). "Design of the Normandie Bridge." *Proceedings of the International Conference on Cable-Stayed and Suspension Bridges*, IABSE, Vol. 1, 605–630.

Watson, S.C., and D. Stafford (1988). "Cables in Trouble." *Civil Engineering*, ASCE, **58**(4), 38–41.

Wei, S.T., and C. Pierre (1988). "Localization Phenomena on Mistuned Assemblies with Cyclic Symmetry, Part I: Free Vibrations." ASME Journal of Vibration and Acoustics, **111**(4), 429–438.

Xu, Y.L., and Z. Yu (1998a). "Vibration of Inclined Sag Cables with Oil Dampers in Cable-Stayed Bridges." *Journal of Bridge Engineering*, **3**(4), 194–203.

Xu, Y.L., and Z. Yu (1998b). "Mitigation of Three-Dimensional Vibration of Inclined Sag Cable using Discrete Oil Dampers — II. Application." *Journal of Sound and Vibration*, **214**(4), 675–693.

Xu, Y.L., Z. Yu, and J.M. Ko (1998c). "Forced Vibration Studies of Sagged Cables with Oil Damper Using the Hybrid Method." *Engineering Structures*, **20**(8), 692–705.

Yamaguchi, H., and R. Adhikari (1995). "Energy-Based Evaluation of Modal Damping in Structural Cables with and without Damping Treatment." *Journal of Sound and Vibration*, **181**(1), 71–83.

Yamaguchi, H., and Y. Fujino (1998). "Stayed Cable Dynamics and its Vibration Control." In Larsen and Esdahl, eds., *Bridge Aerodynamics*, Balkema, Rotterdam, 235–253.

Yoshimura, T., T. Tanaka, N. Sasaki, S. Nakatani, and S. Higa (1988). "Rein-wind Induced Vibration of the Cables of the Aratsu Bridge." *Tenth National Symposium on Wind Engineering*, JAWE, Tokyo, Japan, 127–134.

Yoshimura, T., A. Inoue, K. Kaji, and M. Savage (1989). "A Study on the Aerodynamic Stability of the Aratsu Bridge." *Proceedings of the Canada-Japan Workshop on Bridge Aerodynamics*, Ottawa, Canada, 41–50.